ELSEVIER

www.elsevier.nl/locate/ica

Inorganica Chimica Acta 318 (2001) 53–60

Inorganica Chimica Acta

# Synthesis and photophysical properties of luminescent rhenium(I) and manganese(I) polypyridine complexes containing pendant 1,3,4-oxadiazole/triarylamine assemblies

Youngjin Kim, Frederik W.M. Vanhelmont, Charlotte L. Stern, Joseph T. Hupp *

*Department of Chemistry, Northwestern University, 2145 Sheridan Road, Evanston, IL 60208-3113, USA*

Received 10 October 2000; accepted 20 February 2001

**Abstract**

A strongly absorbing and significantly luminescing diimine ligand, *N*,*N*′-diphenyl-*p*-(benzyl-1,3,4-oxadiazole)-2,2′-bipyridine (DPO-bpy), incorporating π-conjugated oxadiazole linkage units and remote triphenylamine groups has been synthesized and characterized, as have the corresponding mononuclear metal complexes, *fac*-(DPO-bpy)$Re(CO)_3Cl$ and *fac*-(DPO-bpy)$Mn(CO)_3Br$. The rhenium complex was structurally characterized via X-ray crystallography. The nature of the emitting state of each of the complexes was elucidated via transient DC photoconductivity (TDCP), a technique that reports on the sign and magnitude of the difference in dipole moments between the emissive state and ground state. The TDCP signal is negative for the Re complex and is consistent with emission from a metal-to-ligand charge-transfer state. On the other hand, the TDCP signals for the Mn complex and for the free ligand are positive, with the complex yielding the larger value. The TDCP results, as well as extended Hückel calculations, support an intraligand charge-transfer assignment for the emissive states of both the Mn complex and the free ligand, with the former displaying a significantly higher emission quantum yield. © 2001 Published by Elsevier Science B.V.

*Keywords:* Luminescence; Rhenium complexes; Polypyridine complexes; Photoconductivity

## 1. Introduction

Over the past decade, considerable effort has been made in the synthesis of nonlinear optical (NLO) chromophores and their incorporation into polymer matrices to develop organic polymer-based electro-optical materials [1]. NLO chromophore molecules generally feature a segment of extended conjugation containing an electron-donating group (for example, *N*,*N*′-alkylamino or *N*,*N*′-diarylamino) at one end and an electron-accepting group (for example, nitroaromatic) at the other. Qualitatively similar features (good electron-donating and -accepting groups, and good electronic communication) characterize many emissive, visible-region, charge-transfer chromophores of potential value in solar energy conversion schemes. Recently there has been interest on both fronts in transition-metal-based chromophores with polymeric or oligomeric organic chromophores featuring extended conjugation [2]. The issues of interest in these studies have to do with achieving extended charge-transfer and greater electronic excited-state delocalization, either via synergistic chromophoric corporation, or parent excited-state mixing. Potentially useful could be excited-state lifetime extension (leading to improved energy conversion) and/or greater second-order NLO efficiency (due, for exam-

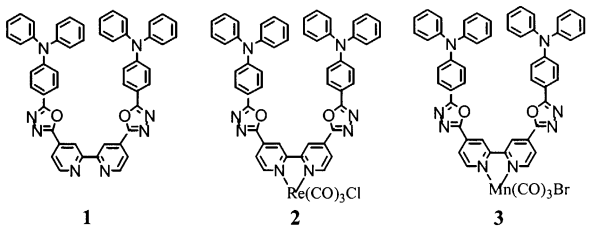


1 2 3

Scheme 1

* Corresponding author. Tel.: +1-847-491 3504; fax: +1-847-491 7713.

*E-mail address:* jthupp@chem.nwu.edu (J.T. Hupp).

0020-1693/01/$ - see front matter © 2001 Published by Elsevier Science B.V.
PII: S0020-1693(01)00400-5

ple, to larger transition-dipole moments, greater ground-state/excited-state changes in molecular dipole moments, or absorption spectral shifting resulting in greater pre-resonance signal enhancement).

We report here on the synthesis and photophysical characterization of a chelating-ligand-functionalized organic chromophore, *N*,*N*′-diphenyl-*p*-(benzyl-1,3,4-oxadiazole)-2,2′-bipyridine (DPO-bpy) (**1**). We also describe the use of the compound as a primary component of a metal-to-ligand charge-transfer (MLCT) type chromophore, *fac*-(DPO-bpy)$Re(CO)_3Cl$ (**2**). Additionally described is the synthesis and photophysical characterization of *fac*-(DPO-bpy)$Mn(CO)_3Br$ (**3**). The manganese compound lacks low-lying MLCT excited states. It represents a useful system, therefore, for evaluating the behavior and properties of the DPO-bpy chromophore in a proximal coordination environment, but without chromophoric interference from the coordination compound itself (Scheme 1).

As background, we note that aromatic oxadiazole-based compounds have attracted particular attention in the context of research on organic light-emitting diodes (LED). The oxadiazoles feature high electron affinities, which in turn, facilitate both electron injection and transport processes of importance in molecular and polymeric LED devices [3–5]. Indeed, polymers containing oxadiazole units have been widely used in experimental devices as both electron-transporting and hole-blocking materials [6]. Saito [7] and others [8,9] have reported that the 1,3,4-oxadiazole ring can be used as an efficient electron-transport moiety for obtaining strong electroluminescence in light-emitting diodes.

Polypyridyl complexes of Re(I) are known to exhibit interesting excited-state electron and energy-transfer properties due to long-lived, emissive MLCT state population [10–15]. The complexes are remarkably photochemically stable and sufficiently chromophorically interesting to have attracted attention both as photonic energy harvesters in proof-of-concept solar cells [16–18] and as emissive reporters in molecule-based chemical sensors [19,20].

As part of the current study we describe how transient DC photoconductivity (TDCP) measurements can be used to elucidate the nature of the emissive excited-states of the chromophoric ligand and the two coordination compounds. Also reported are low-level electronic structure calculations (extended Hückel) that both corroborate and clarify the TDCP findings.

## 2. Experimental

### 2.1. Materials

Synthesis of the oxadiazole derivative, 4-tetrazolytriphenylamine, was accomplished via a published method [9]. 4,4′-Dimethyl-2,2′-bipyridine was purchased from Fluka, $Re(CO)_5Cl$ and $Mn(CO)_5Br$ were purchased from Aldrich Chemical Co. All other reagents were ACS grade and were used without further purification. 2,2′-Bipyridine-4,4′-dicarbonyl chloride was prepared by modifying a published method [21] as indicated below.

#### 2.1.1. Preparation of 2,2′-bipyridine-4,4′-dicarbonyl chloride

4,4′-Dimethyl-2,2′-bipyridine (8.0 g, 43 mmol) was dissolved in concentrated $H_2SO_4$ (100 ml). After the solution was cooled to 0°C, $CrO_3$ (26 g, 260 mmol, 6 equiv.) was added in small portions during 1 h. The mixture, which turned blue-green, was heated to 75°C for 4 h, stirred 10 h at room temperature, and finally poured into a mixture of ice–water. The green precipitate was filtered and washed several times with water. This green powder was then suspended in water, and KOH was added under vigorous stirring until the solution was basic. The blue insoluble residues were filtered and washed with water. The aqueous filtrate was acidified with HCl in order to precipitate the diacid compound. The solid was filtered, washed with water, methanol, and diethyl ether, and dried in vacuo. The resulting 4,4′-dicarboxylic acid-2,2′-bipyridine (1.67 g, 6.84 mmol) was then refluxed with thionyl chloride (20 ml) for 5 h. The solvent was removed by rotary evaporation. The crude product (an oily solid) was extracted with benzene from which a yellow microcrystalline product was recovered. Yield: 1.6 g (83%). $^1H$ NMR (DMSO-$d_6$, $\delta$ ppm): 7.92 (s, 1H), 8.85 (s, 1H), 8.92 (s, 1H). $^{13}C$ NMR (DMSO-$d_6$, $\delta$ ppm): 19.47, 123.41, 139.41, 150.40, 155.08, 165.69. ES MS; $m/z$: 281 [$M^+$].

#### 2.1.2. Preparation of *N*,*N*′-diphenyl-*p*-(benzyl-1,3,4-oxadiazole)-2,2′-bipyridine (DPO-bpy)

A mixture of 2,2′-bipyridine-4,4′-dicarbonyl chloride (0.32 g, 1.14 mmol), 4-tetrazolytriphenylamine (0.882 g, 2.8 mmol), and dry pyridine (30 ml) was refluxed for 2 days under a nitrogen atmosphere. After cooling, the reaction mixture was poured into water, and then filtered to collect the solid. The crude product was recrystallized from a mixture of $CH_2Cl_2$–EtOH. Yield: 0.78 g (87%). $^1H$ NMR ($CHCl_3$-$d_3$, $\delta$ ppm): 9.14 (s, 2H), 8.94 (d, 2H, $J = 4.8$ Hz), 8.13 (d, 2H, $J = 4.8$ Hz), 8.03 (d, 4H, $J = 8.8$ Hz), 7.36 (m, 4H), 7.21 (m, 12H), 7.14 (d, 4H, $J = 8.8$ Hz). $^{13}C$ NMR ($CHCl_3$-$d_3$, $\delta$ ppm): 165.7, 162.4, 156.5, 151.5, 150.4, 146.6, 132.6, 129.8, 128.5, 126.0, 124.8, 120.9, 118.0, 115.3. ES MS; $m/z$: 779 [$M^+$]. *Anal.* Found: C, 76.95; H, 4.27; N, 14.30. Calc. for $C_{50}H_{34}N_8O_2$: C, 77.06; H, 4.36; N, 14.38%.

#### 2.1.3. Preparation of fac-(DPO-bpy)$Re(CO)_3Cl$

A mixture of $Re(CO)_5Cl$ (75.2 mg, 0.21 mmol) and DPO-bpy (162 mg, 0.21 mmol) in dry toluene (20 ml)

was heated to reflux under a nitrogen atmosphere for 1 h. After cooling, the product — an orange–red solid — was collected by filtration, washed with n-hexane, and dried in vacuo. Yield: 0.19 g (83%). $^1$H NMR ($CDCl_3$, $\delta$ ppm) 9.28 (d, 2H, $J = 5.2$ Hz), 9.08 (s, 2H), 8.21 (d, 2H, $J = 5.6$ Hz), 8.08 (d, 4H, $J = 8.4$ Hz), 7.44 (m, 4H), 7.25 (m, 12H), 7.19 (d, 4H, $J = 8.4$ Hz). $^{13}$C NMR ($CDCl_3$, $\delta$ ppm) 196.6, 166.8, 160.4, 156.3, 154.2, 152.1, 146.3, 134.1, 129.9, 129.2, 128.9, 126.4, 126.0, 125.5, 125.2, 123.6, 120.5, 120.3, 114.1. FAB MS; $m/z$: 1085.1 [$M^+$], 1049 [$M^+ - Cl$]. IR (KBr pellet, $cm^{-1}$): $\nu$(CO) 2022, 1922, 1902. *Anal.* Found: C, 58.65; H, 3.18; N, 10.33. Calc. for $C_{53}H_{34}N_8O_5ClRe$ $1.2CH_3CN$: C, 58.70; H, 3.14; N, 10.34%.

Slow diffusion of diethyl ether into an acetonitrile solution of (DPO-bpy)$Re(CO)_3Cl$ afforded orange-red crystals suitable for X-ray crystallographic studies.

#### 2.1.4. Preparation of *fac*-(DPO-bpy)$Mn(CO)_3Br$

A mixture of $Mn(CO)_5Br$ (0.137 g, 0.5 mmol) and DPO-bpy (0.388 g, 0.5 mmol) in deaerated dry toluene–THF (20 ml) was refluxed under $N_2$ atmosphere for 1.5 h. After cooling, a yellow–orange solid was collected by filtration, washed with cold diethyl ether, and dried in vacuo. The crude product was recrystallized from acetonitrile–THF. Yield: 0.419 g (86%). $^1$H NMR ($CD_2Cl_2$, $\delta$ ppm) 8.76 (d, 2H, $J = 5.6$ Hz), 8.63 (d, 2H, $J = 5.8$ Hz), 8.56 (d, 2H, $J = 5.6$ Hz), 7.87 (d, 2H, $J = 5.2$ Hz), 7.31 (m, 4H), 7.20 (m, 12 H), 6.87 (d, 4H, $J = 8.4$ Hz). $^{13}$C NMR ($CD_2Cl_2$, $\delta$ ppm) 209.8, 192.7, 167.2, 160.8, 155.3, 154.1, 151.8, 148.3, 145.4, 140.8, 132.9, 131.9, 130.5, 129.1, 125.7, 124.4, 121.2, 119.6, 116.8. FAB MS; $m/z$: 998.6 [$M^+$], 918 [$M^+ -$ Br]. IR (KBr pellet, $cm^{-1}$): $\nu$(CO) 2026, 1940, 1923. *Anal.* Found: C, 63.74; H, 3.47; N, 11.21. Calc. for $C_{53}H_{34}N_8O_5BrMn$: C, 63.82; H, 3.41; N, 11.24%.

### 2.2. Measurements

Electronic absorption spectra were obtained by using a HP 8452A diode array spectrophotometer. IR spectra (KBr pellets) were obtained by using a Bio-Rad FTIR spectrophotometer. Steady-state emission spectra were obtained using an ISA Fluorolog Model FL3-11 spectrophotometer, and luminescence quantum yields were determined at room temperature by using samples of low absorbance (Abs. $< 0.12$). The integrated emission profiles were compared to that of a standard sample of $Ru(bpy)_3^{2+}$ in deoxygenated acetonitrile ($\varphi_{em} = 0.062$) [13]. Emission lifetimes were obtained by using a Photon Technologies International Timemaster spectroscopic detection instrument with a gated nitrogen lamp (337 nm excitation, $\pm 1.0$ ns resolution). For the TDCP measurements saturated solutions of all compounds in deoxygenated chloroform were filtered through a Teflon filter (0.22 μm) and diluted 1:1 with toluene prior to use. The measurements were performed in a cell featuring stainless steel electrodes. A voltage of 1000 V was applied over the 0.46 mm gap. The excitation wavelength was 420 nm and was produced by an OPOTEK Vibrant tunable laser system pumped by the third harmonic of a Quantel Brillant Nd:YAG Laser. Laser pulse widths were approximately 4–5 ns. The laser intensity at the cell was typically 150–250 μJ $pulse^{-1}$. Extended Hückel calculations were performed on *fac*-(DPO-bpy)$Re(CO)_3Cl$ and *fac*-(DPO-bpy)$Mn(CO)_3Br$ using HyperChem software (version 5.11 Pro for Windows, Hypercube, Inc., Gainesville, FL).

### 2.3. X-ray crystallography

A red block crystal of $C_{55.50}H_{38}N_9O_6ClRe$ having approximate dimensions of $0.23 \times 0.14 \times 0.07$ $mm^3$ was mounted on a glass fiber. All measurements were made on a SMART-1000 CCD area detector with graphite monochromated Mo Kα radiation. Cell constants and an orientation matrix for data collection corresponded to a primitive triclinic cell with dimensions: $a = 10.557$ (2), $b = 11.051$ (3), $c = 23.363$ (5) Å, $\alpha = 81.750$ (4), $\beta = 89.696$ (4), $\gamma = 70.261$ (4)°, $V = 2536.3$ (9) Å$^3$. For $Z = 2$ and FW = 1148.63, the calculated density is 1.50 g $cm^{-3}$. Based on a statistical analysis of intensity distribution, and the successful solution and refinement of the structure, the space group was determined to be $P\bar{1}$ (No. 2).

The data were collected at a temperature of $-120 \pm 1$°C to a maximum $2\theta$ value of 56.7°. Data were collected in 0.30° oscillations with 25.0 s exposures. The crystal-to-detector distance was 50.00 mm and the detector swing angle was 28.00°. Of the 23 383 reflections which were collected, 11 725 were unique ($R_{int} = 0.040$); equivalent reflections were merged. Data were collected and processed using the SMART-NT and SAINT-NT programs (Bruker). The linear absorption coefficient, $\mu$, for Mo Kα radiation is 25.1 $cm^{-1}$. An empirical absorption correction was applied. Maximum and minimum effective transmission factors were 1.000000 and 0.732261, respectively. The data were corrected for Lorentz and polarization effects. The structure was solved by direct methods [22] and expanded using Fourier techniques [23]. The solvent acetonitrile, methanol and water molecules were refined isotropically, while the remaining non-hydrogen atoms were refined anisotropically. Hydrogen atoms were included except on the solvent molecules, but not refined. The final cycles of full-matrix least-squares refinement, $\Sigma w(F_o^2 - F_c^2)^2$ on $F^2$ was based on 5556 observed reflections and 649 variable parameters and converged (largest parameter shift was 0.04 times its e.s.d) with unweighted and weighted agreement factors of

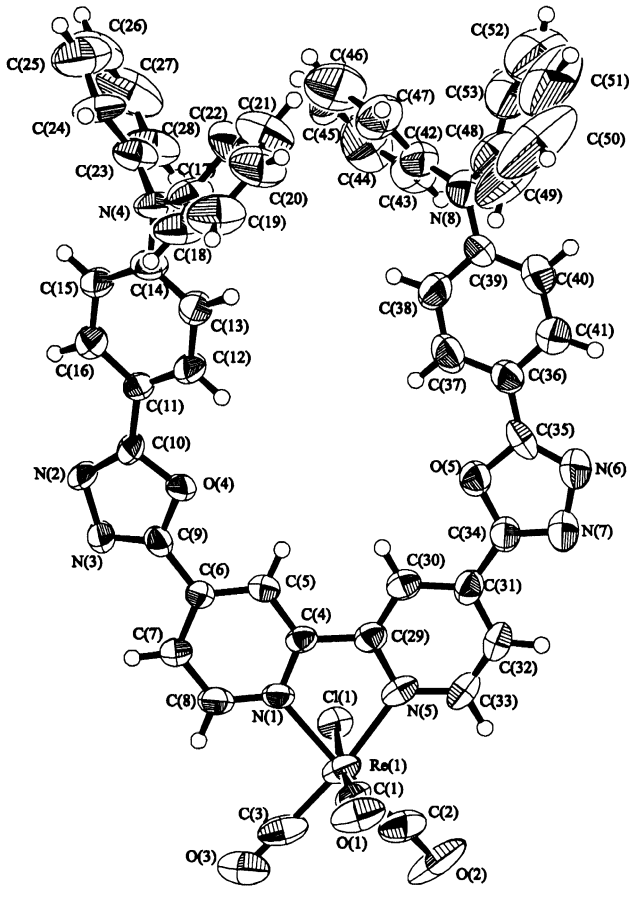


Fig. 1. Perspective drawing of the complex *fac*-(DPO-bpy)Re(CO)$_3$Cl with atomic numbering scheme. Hydrogen atoms have been omitted for clarity. The thermal ellipsoids are shown at the 50% probability levels.

Table 1
Selected bond distances (Å) and bond angles (°) for complex *fac*-(DPO-bpy)Re(CO)$_3$Cl

| | | | |
|---|---|---|---|
| *Bond distances* | | | |
| Re–CL(1) | 2.451(3) | Re–C(1) | 1.909(12) |
| Re–N(1) | 2.150(7) | Re–C(2) | 1.904(13) |
| Re–N(5) | 2.161(8) | Re–C(3) | 1.863(13) |
| *Bond angles* | | | |
| CL(1)–Re–N(1) | 83.2(2) | CL(1)–Re–N(5) | 86.2(2) |
| CL(1)–Re–C(1) | 172.6(4) | CL(1)–Re–C(2) | 90.7(3) |
| CL(1)–Re–C(3) | 95.2(3) | N(1)–Re–N(5) | 74.8(3) |
| N(1)–Re–C(1) | 94.7(4) | N(1)–Re–C(2) | 172.7(4) |
| N(1)–Re–C(3) | 97.6(4) | N(5)–Re–C(1) | 86.4(4) |
| N(5)–Re–C(2) | 100.8(4) | N(5)–Re–C(3) | 172.1(4) |
| C(1)–Re–C(2) | 90.8(5) | C(1)–Re–C(3) | 92.1(5) |
| C(2)–Re–C(3) | 86.9(5) | | |

$R = 0.052$ and $R_w = 0.096$. The value of the goodness-of-fit parameter was 2.20. The weighting scheme was based on counting statistics. The plots of $\Sigma w(|F_o| - |F_c|)^2$ versus $|F_o|$, reflection order in data collection, $\sin\theta/\lambda$ and various classes of indices showed no unusual trends. The maximum and minimum peaks on the final difference Fourier map corresponded to 1.73 and $-1.07$ e Å$^{-3}$, respectively, and were located near the Re position. All calculations were performed using the TEXSAN crystallographic software package of Molecular Structure Corporation.

## 3. Results and discussion

### 3.1. Synthesis and preliminary characterization

FAB mass spectra, elemental analysis, and $^1$H NMR data are consistent with the proposed formulations for the ligand and its metal complexes. IR spectra for both complexes show three intense absorption bands in the region 1850–2080 cm$^{-1}$, as expected for facial configurations of the carbonyl groups [24].

### 3.2. X-ray crystal structure

The proposed structure of (DPO-bpy)Re(CO)$_3$Cl was confirmed via single-crystal X-ray structural studies. An ORTEP drawing of the structure with atomic numbering is shown in Fig. 1. The coordination geometry at the Re atom is distorted octahedral with the carbonyl ligands arranged in a facial fashion. The six aromatic rings (two pyridine, two 1,3,4-oxadiazole and two phenyl rings) are nearly coplanar: the dihedral angle between the least-squares plane of the pyridine and the 1,3,4-oxadiazole ring is 16.40 (6.73)° and between the 1,3,4-oxadiazole and the phenyl rings is 9.38 (4.26)°.[1] Selected crystallographic data are presented in Table 1. Further details are given in Section 5.

### 3.3. Photophysical behavior: absorption and emission

Electronic absorption and emission spectra for the free ligand, *fac*-(DPO-bpy)Re(CO)$_3$Cl, and *fac*-(DPO-bpy)Mn(CO)$_3$Br complexes are shown in Fig. 2; photophysical data are summarized in Table 2. The free ligand shows an intense absorption band in the 380 nm region and displays a broad emission centered at 512 nm. The emission lifetime at room temperature is $6 \pm 1$ ns, consistent with an assignment as fluorescence from an intraligand excited-state. As shown below, the emitting state possesses significant charge-transfer character. The absorption spectrum of (DPO-bpy)Re(CO)$_3$Cl shows several intense bands in the 300–380 nm region, attributable to DPO-bpy centered transitions and a weaker band at 450 nm, which is attributed to a nominally singlet MLCT transition ($d_\pi(Re) \rightarrow \pi^*$(diimine)). The room-temperature emission maxi-

[1] The first value is for the rings on the left-hand side of the molecule as depicted in Fig. 1. The value in brackets is for the rings on the right-hand side.

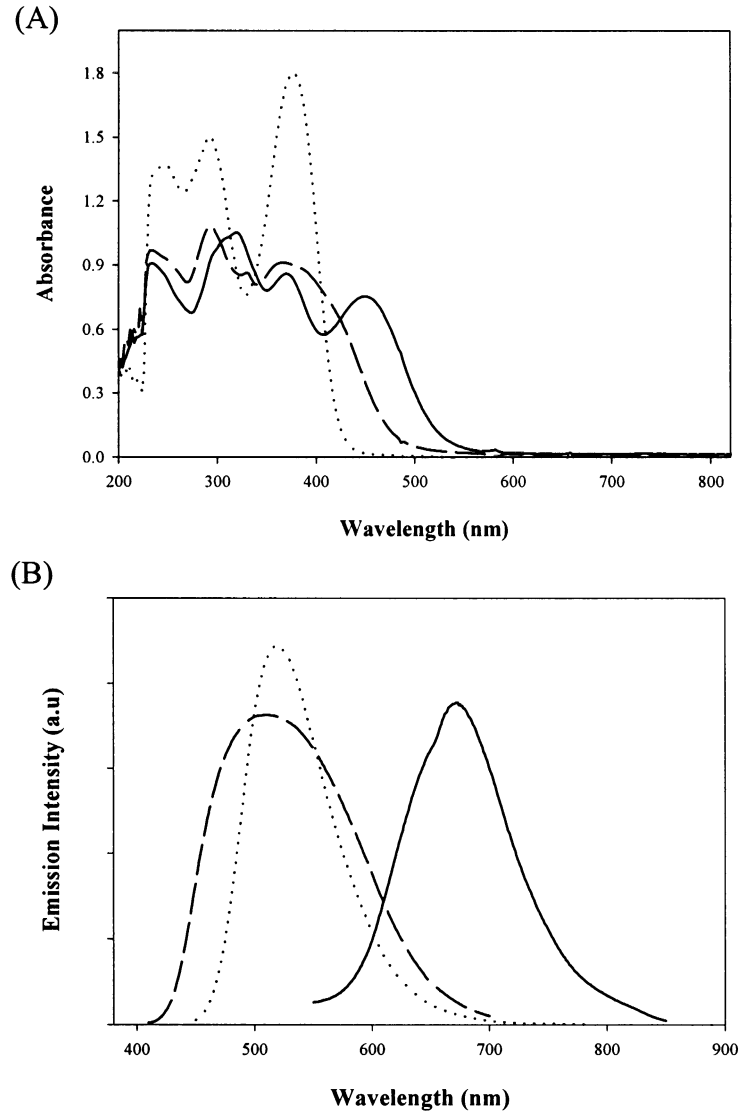


Fig. 2. (A) Electronic absorption; and (B) corrected emission spectra in deoxygenated $CH_2Cl_2$ at room temperature for *fac*-(DPO-bpy)$Re(CO)_3Cl$ (—), *fac*-(DPO-bpy)$Mn(CO)_3Br$ (- - -), and free DPO-bpy (· · ·).

Table 2
Spectral and photophysical data [a]

| Compound | $\lambda_{max}$ (nm) [b] [$10^{-3}$ $\varepsilon$ ($dm^3\ mol^{-1}\ cm^{-1}$)] | $\lambda_{max,em}$ (nm) | $\varphi_{em}$ [c] | $\tau$ (ns) | $\Delta\mu_{eff}$ [d] (debye) |
|---|---|---|---|---|---|
| DPO-bpy | 380 (107) | 512 | 0.02 | $6 \pm 1$ | +8 |
| (DPO-bpy)$Re(CO)_3Cl$ | 450 (29)<br>378 (32) | 672 | 0.05 | $18 \pm 1$ | −6 |
| (DPO-bpy)$Mn(CO)_3Br$ | 378 (53)<br>410 (sh) | 519 | 0.14 | $7 \pm 1$ | +12 |

[a] Emission and TDCP data obtained from deoxygenated methylene chloride solution at room temperature.
[b] Only the lowest energy maximum or shoulder is reported.
[c] $\varphi_{em}$ values were calculated by referencing against values at 298 K ($\varphi_r$) by using equation, $\varphi_{em} = \varphi_r(B_r/B_s)(n_s/n_r)^2(D_s/D_r)$, $B = (1-10^{-A})$: $\varphi_r = 0.062$ for standard sample (see Ref. [13]); $D$, the integerated intensity; $n$, refractive index; $A$, the absorption at the excitation wavelength. $\lambda_{max,em}$ is corrected emission maximum and $\varphi_{em}$, the quantum yield for emission.
[d] $\Delta\mu_{eff} = (\mu_{ex}{}^2 - \mu_g{}^2)^{1/2}$.

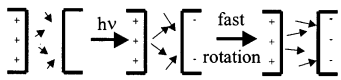


Scheme 2

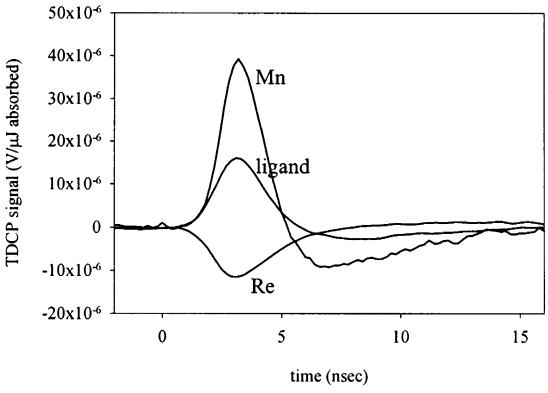


Fig. 3. TDCP response normalized for absorbed energy from deoxygenated $CHCl_3$–toluene solutions of *fac*-(DPO-bpy)$Re(CO)_3Cl$, *fac*-(DPO-bpy)$Mn(CO)_3Br$, and free DPO-bpy.

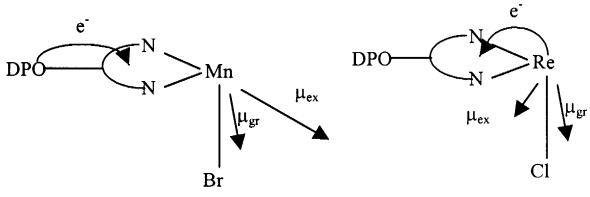


Scheme 3

mum occurs at 672 nm. The substantial emission red-shift for the complex in comparison to the free ligand strongly suggests a $^3$MLCT emitting state for the complex, and indeed, the emission energy is broadly consistent with that observed for diimine tricarbonyl chloride complexes of Re(I) [12]. On the other hand, an argument might be made for an intraligand assignment: chelation of a metal cation could render the diimine nitrogens better electron acceptors. This would induce red shifts in both the absorption and emission spectra. We have noted elsewhere that such effects can, in certain cases, be rather substantial [25]. Emission lifetime studies yielded $\tau = 18$ ns, a value that arguably could be consistent with either an MLCT or intraligand CT assignment. Given the ambiguity, we reasoned that the assignment could be clarified by assembling a metal complex that largely reproduced the physical structure of (DPO-bpy)$Re(CO)_3Cl$, but lacked energetically accessible MLCT transitions. By offering low-energy, filled 3dπ metal orbitals in place of high-energy, filled 5dπ metal orbitals, the complex, (DPO-bpy)Mn-$(CO)_3Br$, satisfies these conditions. As shown in Fig. 2 and Table 2, the manganese compound emits at nearly the same energy as the free ligand, but considerably to the blue of the rhenium compound. From the various comparisons we conclude that $^3$MLCT emission, rather than intraligand CT emission, is responsible for the luminescence of the rhenium complex.

### 3.4. Photophysical behavior: TDCP

TDCP is a technique that provides information about the sign and magnitude of differences in dipole moment, $\mu$, for the ground state versus an excited state of an uncharged molecular chromophore in solution [26].

A static, external electric field is applied in the cell in order to orient the dipolar molecules, as shown in Scheme 2. If the dipole moment changes upon photoexcitation, the chromophores will become either more completely (increase in $|\mu|$) or less completely (decrease in $|\mu|$) oriented by the external field. The reorientation and associated build up of charge can be tracked by monitoring the transient photovoltage generated across the TDCP cell. Braun and Smirnov, in particular, have shown how the TDCP methodology can be utilized to: (a) evaluate the degree of photo-induced charge transfer; (b) measure net electron-transfer distances; and/or (c) monitor excited-state rotational correlation times for various light-absorbing organic compounds [26]. We have recently applied the technique to simple inorganic chromophores [27,28].

Fig. 3 shows the TDCP responses of the free ligand and complexes. Notably, the signal at short and intermediate times after the laser pulse is negative for the Re complex, but positive for the Mn complex and the free ligand. This indicates that the emissive excited-state has a smaller dipole moment than the ground state for the Re sample and vice versa for the ligand and the Mn sample. Negative signals have also been observed for (bipyridine)$Re(CO)_3Cl$ [27] and a series of related complexes [29], all of which emit from $^3$MLCT excited-states.

As illustrated in Scheme 3 and described in greater detail elsewhere [27], the Re(I)–halide bond creates a substantial ground-state dipole moment. While giving rise to a smaller dipole contribution associated with the Re–diimine fragment, MLCT excitation all but eliminates the Re–X contribution to the molecular dipole moment. The net result is a decrease in overall molecular dipole moment, where the decrease is detectable as a negative TDCP signal.

Since the sign of the TDCP signal for the Mn complex is *positive*, it is clear that this complex (and the free ligand) must be emitting from a different state. The sign is consistent with the proposed intraligand charge-transfer assignment. Notably, the TDCP signal amplitude is larger for the Mn complex than for the free ligand. The difference likely primarily reflects differences in ground-state dipole moments, $\mu_g$, rather than

differences in the change in dipole moment, $\mu_{ex} - \mu_g$. Note that the TDCP signals scale as $\mu_{ex}{}^2 - \mu_g{}^2$, not $\mu_{ex} - \mu_g$. The Mn complex should possess a substantial $\mu_g$ value due to the strong dipolar character of the Mn(I)–bromide bond. Furthermore, this contribution should be largely unaffected by intraligand charge-transfer excitation. Thus, in the emissive excited-state, intraligand CT and Mn–X dipole contributions (vector quantities) should be partially additive, thereby generating a very substantial $\mu_{ex}$ value; see Scheme 2. In the absence of independent information about $\mu_g$, however, it is not possible to estimate $\mu_{ex}$ values from the TDCP measurements. Instead, in Table 2 we have reported 'effective' dipole moment changes, $\Delta\mu_{eff}$, given by the square root of $(\mu_{ex}{}^2 - \mu_g{}^2)$.

Finally, returning to the Re complex, we note that an alternative excited-state description — one in which reductive quenching (electron transfer from the aryl amine to the metal center) occurs very shortly after MLCT excited-state formation [14b] — can be ruled out on the basis of the sign of the TDCP signal for this compound. The reductively quenched form of the compound should resemble the intraligand CT state generated within the Mn complex and yield a positive, rather than negative, TDCP signal. The measurement, however, does not eliminate the possibility that quenching shortens a longer-lived MLCT excited-state to 18 ns. The TDCP results would require the putative amine/bpy CT state, however, to be very short-lived, since post-MLCT evidence for it is not obtained in the conductivity experiment.

### 3.5. Electronic structure calculations

Consistent with emission from an intraligand CT state, extended Hückel calculations for the Mn complex reveal that the HOMO is located primarily on the nitrogens of the diphenylamino groups, whereas the LUMO is centered on the bipyridine portion of the ligand. The highest filled orbital with substantial Mn character is the HOMO-30 (2.1 eV below the HOMO), obviously making MLCT excited-states inaccessible. According to the extended Hückel calculations, the highest lying filled orbital with substantial metal character in the rhenium complex, on the other hand, is the HOMO-2. Higher quality calculations presumably would slightly alter the orbital ordering, making a metal orbital the HOMO, as implied by the available experimental results.

### 3.6. Applications

Improved dye-sensitization of semiconductor-based liquid-junction solar cells, enhanced second-order nonlinear optical behavior, and enhanced performance of molecule-based light emitting diodes are among the long-range applications-based motivations for investigating the photophysical properties of intentionally combined inorganic/organic chromophore pairs. With preliminary results in hand for the (DPO-bpy)$M(CO)_3X$ compounds, we consider, in order, the candidate applications. *N*,*N*′-diphenyl-*p*-benzyl-1,3,4-oxadiazole attachment clearly extends the spectral range of (bpy)$Re(CO)_3Cl$, with the DPO moiety functioning as an antenna for population of a $^3$MLCT state of the inorganic chromophore. The added chromophoric coverage, however, occurs in the near-UV region. Enhanced chromophoric behavior here is of little practical value for metal-oxide semiconductor-based solar cells [17,30] (e.g. 'Grätzel cells') because of the low near-UV content of the solar radiation reaching the earth's surface and because of the ability of the semiconductors themselves to absorb photons in the near-UV region.

DPO attachment to (bpy)$Re(CO)_3Cl$ yields an intense intraligand charge-transfer absorption band. The existence of a strongly allowed pre- or post-resonant charge-transfer transition is a prerequisite for efficient frequency doubling (i.e. second-order NLO behavior) by materials composed of aligned molecular chromophores. Since (bpy)$Re(CO)_3Cl$ itself displays a modest propensity for frequency doubling [31,32], presumably due primarily to the existence of allowed MLCT transitions, the addition of intense ligand-based CT transitions to the linear absorption spectrum might be expected to yield very substantial improvements in doubling efficiency. This would be reflected, for example, in an increase in the absolute magnitude of the wavelength-dependent molecular first hyperpolarizability, $\beta$. Unfortunately, because $\beta$ is a signed quantity, and because the transition-dipole moments for the MLCT and intraligand CT excitations are largely antiparallel, the contributions to $\beta$ from these two transitions should be oppositely signed and, therefore, partially canceling, under pre-resonance conditions (nonabsorbing conditions).

Finally, from Table 2, the addition of $Re(CO)_3Cl$ to DPO-bpy yields a modest increase in photoluminescence quantum yield. A corresponding increase in the quantum yield for electroluminescence might be expected. Unfortunately, the increase comes at the expense of a likely undesirable red-shift of the emission. The addition of $Mn(CO)_3Br$, on the other hand, leaves the emission energy largely unaffected, but boosts the quantum yield for photoluminescence by nearly an order of magnitude — an obviously positive outcome if parallelled in electroluminescence experiments. In view of the essentially identical emission lifetimes for the free ligand and the manganese complex, the enhancement in quantum yield clearly is a consequence of an increase in the excited-state radiative decay rate rather than a decrease in the nonradiative rate.

## 4. Conclusions

The combination of a pair of triarylamines with 2,2′-bipyridine via oxadiazole linkages yields, upon coordination to manganese or rhenium, a nearly coplanar six-ring assembly. The free assembly luminesces from an intraligand charge-transfer state, where the CT character of the state was established via transient DC photoconductivity measurements. Despite the pendant triarylamine — a potential reductive quencher — the rhenium tricarbonylchloro complex of the assembly readily emits in solution from a $^3$MLCT excited-state featuring a lifetime of $\sim$18 ns at ambient temperature. The MLCT assignment is supported by TDCP data. The corresponding manganese tricarbonylbromo complex emits from an intraligand excited-state where the quantum yield for emission is about seven times that for the free ligand.

## 5. Supplementary material

Tables of crystal data, structure solution and refinement, atomic coordinates, bond lengths and angles, least-squares planes, and anisotropic thermal parameters for *fac*-(DPO-bpy)Re(CO)$_3$Cl complex (PDF) and X-ray crystallographic files in CIF format for Re complex are available from the authors on request.

## Acknowledgements

We thank Professor F. Lewis for the use of the lifetime setup and Dr. Rajdeep Kalgutkar for help with these measurements. Financial support from Swiss National Science Foundation (postdoctoral fellowship for F.W.M.V.) and the Chemical Sciences, Geosciences and Biosciences Division, Office of Basic Energy Sciences, Office of Science US Department of Energy (Grant No. DE-FG02-87ER13808) is gratefully acknowledged.

## References

[1] (a) R. Dagani, Chem. Eng. News 74 (1996) 22. (b) S. Marder, J.W. Perry, Science 263 (1994) 1706. (c) T.J. Marks, M.A. Ratner, Angew. Chem., Int. Ed. Engl. 34 (1995) 155. (d) T. Verbiest, D.M. Burland, M.C. Jurich, V.Y. Lee, R.D. Miller, W. Volksen, Science 268 (1995) 1604.
[2] (a) S.C. Rasmussen, D.W. Thompson, V. Singh, J.D. Petersen, Inorg. Chem. 35 (1996) 3449. (b) Z. Peng, L. Yu, J. Am. Chem. Soc. 118 (1996) 3777.
[3] (a) R.H. Friend, R.W. Gymer, A.B. Holmes, J.H. Burroughes, R.N. Marks, C. Taliani, D.D.C. Bradley, D.A. Dos Santos, J.L. Bredas, M. Logdlund, W.R. Salaneck, Nature 397 (1999) 121. (b) J.H. Burroughes, D.D.C. Bradley, A.R. Brown, R.N. Marks, K. Mackay, R.H. Friend, P.L. Burn, A.B. Holmes, Nature 347 (1990) 539.
[4] M. Strukely, F. Papadimitrakopoulos, T.M. Miller, L.J. Rothberg, Science 267 (1995) 1969.
[5] B. Schulz, M. Bruma, L. Brehmer, Adv. Mater. 9 (1997) 601.
[6] Y. Yang, Q. Pei, J. Appl. Phys. 77 (1995) 4807.
[7] (a) M. Era, T. Tsutsui, S. Saito, Appl. Phys. Lett. 67 (1995) 2436. (b) N. Takada, T. Tsutsui, S. Saito, Appl. Phys. Lett. 63 (1993) 2032.
[8] A. Kraft, Chem. Commun. (1996) 77.
[9] N. Tamoto, C. Adachi, K. Nagai, Chem. Mater. 9 (1997) 1077.
[10] (a) T.D. Westmoreland, K.S. Schanze, P.E. Neveux, J.E. Danielson, B.P. Sullivan, P. Chen, T.J. Meyer, Inorg. Chem. 24 (1985) 2596. (b) P. Chen, E. Danielson, T.J. Meyer, J. Phys. Chem. 92 (1988) 3708.
[11] B.P. Sullivan, J. Phys. Chem. 93 (1989) 24.
[12] L.A. Worl, R. Duesing, P. Chen, L.D. Ciana, T.J. Meyer, J. Chem. Soc., Dalton Trans. (1991) 849.
[13] J.V. Caspar, T.J. Meyer, J. Phys. Chem. 87 (1983) 952.
[14] (a) T.A. Perkins, D.B. Pourreau, T.L. Netzel, K.S. Schanze, J. Phys. Chem. 93 (1989) 4511. (b) Y.S. Wang, B.T. Hanser, M.M. Rooney, R.D. Burton, K.S. Schanze, J. Am. Chem. Soc. 115 (1993) 5675.
[15] (a) K.D. Ley, Y.T. Li, J.V. Johnson, D.H. Powell, K.S. Schanze, Chem. Commun. (1999) 1749. (b) K.D. Ley, K.S. Schanze, Coord. Chem. Rev. 171 (1998) 287. (c) K.D. Ley, C.E. Whittle, M.D. Barberger, K.S. Schanze, J. Am. Chem. Soc. 119 (1997) 3423.
[16] P.-A. Bruuger, M. Grätzel, J. Am. Chem. Soc. 102 (1980) 2461.
[17] B. O'Regan, M. Grätzel, Nature 353 (1991) 737.
[18] B.P. Sullivan, D. Conrad, T.J. Meyer, Inorg. Chem. 24 (1985) 3640.
[19] (a) M.H. Keefe, K.D. Benkstein, J.T. Hupp, Coord. Chem. Rev., in press. (b) K.D. Benkstein, J.T. Hupp, C.L. Stern, J. Am. Chem. Soc. 120 (1998) 12 982. (c) R.V. Slone, K.D. Benkstein, S. Belanger, J.T. Hupp, I.A. Guzei, A.L. Rheingold, Coord. Chem. Rev. 171 (1998) 221.
[20] P.R. Ashton, V. Balzani, O. Kocian, L. Prodi, N. Spencer, J.F. Stoddart, J. Am. Chem. Soc. 120 (1998) 11 190.
[21] K. Piotr, K. Gary, C. Leszek, J. Heterocycl. Chem. 28 (1991) 7.
[22] G.M. Sheldrick, SHELX-97, 1997.
[23] P.T. Beurskens, G. Admiraal, G. Beurskens, W.P. Bosman, R. de Gelder, R. Israel, J.M.M. Smits, The DIRDIF-94 program system, Technical Report of the Crystallography Laboratory, University of Nijmegen, Netherlands.
[24] P.J. Giordano, M.S. Wrighton, J. Am. Chem. Soc. 101 (1979) 2888.
[25] F.W. Vance, J.T. Hupp, J. Am. Chem. Soc. 121 (1999) 4047.
[26] S.N. Smirnov, C.L. Braun, Rev. Sci. Instrum. 69 (1998) 2875 (and references therein).
[27] F.W.M. Vanhelmont, J.T. Hupp, Inorg. Chem. 39 (2000) 1817.
[28] F.W.M. Vanhelmont, R.C. Johnson, J.T. Hupp, Inorg. Chem. 39 (2000) 1814.
[29] Y.-J. Kim, F.W. M. Vanhelmont, J.T. Hupp, submitted for publication.
[30] J.-E. Moser, M. Grätzel, Chimia 52 (1998) 160.
[31] (a) V.W.W. Yam, Y. Yang, H.P. Yang, K.K. Cheung, Organometallics 18 (1999) 5252. (b) A.G. Anderson, J.C. Calabrese, W. Tam, I.D. Williams, Chem. Phys. Lett. 134 (1987) 392. (c) J.C. Calabrese, W. Tam, Chem. Phys. Lett. 133 (1987) 244.
[32] (a) G.J. Ashwell, R.C. Hargreaves, C.E. Baldwin. C.S. Bahra, C.R. Brown, Nature 357 (1992) 393. (b) K. Clays, M. Wu, A. Persoons, J. Nonlinear Opt. Phys. Mater. 5 (1996) 59.